Geometric Methods for Vortex Extraction

I. Ari Sadarjoen* and Frits H. Post

Faculty of Information Technology and Systems, Delft University of Technology,
Zuidplantsoen 4, 2628 BZ Delft, The Netherlands
e-mail: Ari.Sadarjoen@mcc.ac.uk / Frits.Post@cs.tudelft.nl

Abstract. This paper presents two vortex detection methods which are based on the geometric properties of streamlines. Unlike traditional vortex detection methods, which are based on point-samples of physical quantities, one of our methods is also effective in detecting weak vortices. In addition, it allows for quantitative feature extraction by calculating numerical attributes of vortices. Results are presented of applying these methods to CFD simulation data sets.

Keywords: flow visualization, vortex detection, feature extraction

1 Introduction

Vortices are among the most important features of fluid flows. In aerodynamics, vortices directly affect the flying characteristics of airplanes [5]. In turbomachinery design, vortices are to be avoided or minimized during design [9]. In oceanography, the evolution of vortices in space and time is important for scientists' understanding of ocean circulations [14]. Therefore, detecting and visualizing vortices is an important topic. Unfortunately, there is no formal definition of a vortex, which makes it difficult to detect them. Therefore, vortex detection methods are based on heuristic criteria.

Vortex detection methods fall into two classes. The first class is based on physical quantities evaluated at isolated points in the field, e.g. grid nodes, or in an infinitesimal neighbourhoods of points. Examples of these quantities are pressure, vorticity magnitude, and helicity [1, 9]. The problem is that none of these methods works in all cases. Their main deficiency is that they often do not find weak vortices, characterized by slow rotation and low velocity magnitudes.

The second and relatively new class of vortex detection methods are the *geometric methods*, which are not based on physical quantities, but on geometric properties of curves, typically streamlines or pathlines.

The purpose of this paper is to present two geometric methods for vortex detection, and a method for calculating numeric attributes of vortices. The first method tries to find vortex cores by determining the curvature centre of the osculating circle of streamlines through many sample points in the grid. The second method tries to find entire vortices using the winding-angle concept, to select streamlines that are sufficiently rotational to be part of a vortex.

* Present address: Manchester Visualization Centre, Manchester Computing, University of Manchester, Oxford Road, Manchester M13 9PL, United Kingdom

We have extended the work in [12] to a technique for automatic feature extraction, characterizing the features by calculating a set of quantitative attributes, such as position, size, and rotation speed and direction. This is done by clustering the selected streamlines and determining numerical attributes of the vortices. This has the advantage that vortices can be described by a small set of attributes, which naturally causes a dramatic data reduction.

The structure of this paper is as follows. In Section 2, we give an overview of related work. Then, we describe our geometric methods for vortex detection: the curvature centre method in Section 3, and the winding-angle method in Section 4. In Section 5, we show some results of applying our methods to CFD simulations.

2 Related Work

The first class of vortex detection methods is typically based on point samples of physical quantities. The quantities involved are usually pressure, velocity, quantities derived from the velocity vector, or quantities derived from the velocity gradient tensor. All of these quantities are based on the assumption either that vortices are regions with a high amount of rotation, or that there exists a pressure minimum at vortex cores. Banks & Singer [1] and Roth & Peikert [9] have surveyed a number of quantities, and concluded that they often fail to capture all vortices. An important cause is that vortices are *regional* features, but these criteria are strictly based on point samples, or first-order approximations in infinitesimal regions. Recently, Roth & Peikert [10], recognizing the deficiencies of first-order approximations, proposed a higher-order method which is also able to detect bent vortices.

The second class of vortex detection methods is *geometric*, i.e. based on geometric properties of streamlines. De Leeuw [6] described an interactive way to detect vortices using a box-shaped probe in which sample points are taken. For all the sample points in the box, a number of properties were calculated, including the centre of curvature of the streamline through the sample point. When the box contained a vortex, the centres of curvature would accumulate near a point, otherwise they would be scattered.

Portela [7] has developed a formal mathematical framework for defining vortices in 2D, which corresponds to the intuitive notion of swirling motion around a central set of points. To define a central set of points, he proposed so-called Jordan structures; to define swirling motion, he used the winding-angle concept known from differential geometry.

In [12], we applied two geometric techniques to several hydrodynamic cases. One used curvature centres to find vortex cores, the second used a simplified winding-angle.

The present paper reviews the first technique, giving more details on its problems and pitfalls, and extends the second technique to a more quantitative one, by clustering the streamlines and calculating numeric attributes.

3 The Curvature Centre Method

The curvature centre method tries to detect vortices in 2D by sampling the field at many points, typically at all grid nodes. For each sample point, the *centre of curvature* is

determined, which is the centre of the osculating circle of the streamline through that point [2]. In vortical regions of the field, the centres of curvature should accumulate at a point, as in Figure 1a. The samples taken on this perfectly circular streamline all project to the same centre of curvature. In non-vortical regions of the field, the centres of curvature will be scattered, as in Figure 1b.

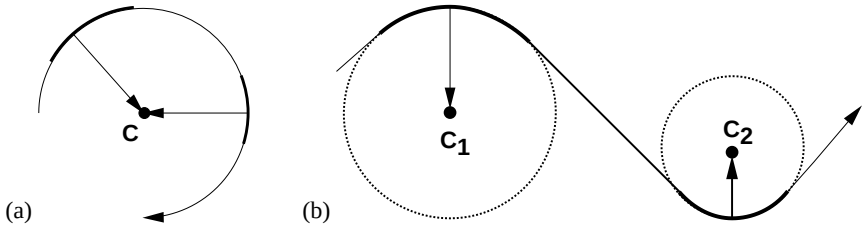

Fig. 1. (a) Circular streamline with coinciding curvature centres C and (b) Non-circular streamline with scattered curvature centres.

In this way, a set of curvature centre points is obtained, which are accumulated into a new grid, as illustrated in Figure 2. The number of curvature centres in each cell constitutes a new scalar field which we call the *Curvature Centre Density* (CCD) field.

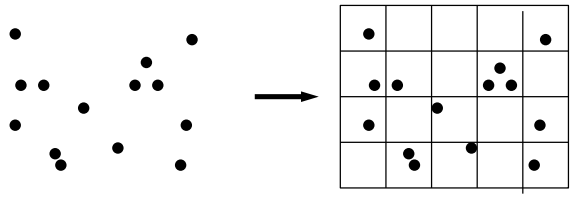

Fig. 2. Curvature centre points are accumulated into a new grid, resulting in the Curvature Centre Density (CCD) scalar field.

Figure 3 shows an example of a CCD field. The 2D data set originates from a numerical flow simulation of the Pacific Ocean, which models the west coast of North America [14]. The grid used is a rectilinear 2D grid of 117×84 nodes, at each of which the velocity has been calculated. The figure shows streamlines released from every grid node. The CCD field has been rendered as a white height field. Thresholding has been applied to select only the highest peaks of the field: $CCD > 0.8 \cdot CCD_{max}$.

This method works, but has the same limitations as traditional point-based detection methods. There are some false and some missing peaks. Some of the false peaks may be filtered out by thresholding or filtering. Also, supersampling may be applied to get more samples per grid cell [11]. An important cause of these problems are the streamlines which are not perfectly circular, but elliptical or elongated; this is often due to interaction between adjacent vortices. The effect is shown in Figure 4: in perfectly circular flow (see Figure 4a), there is a clear peak in the CCD field (see Figure 4b). How-

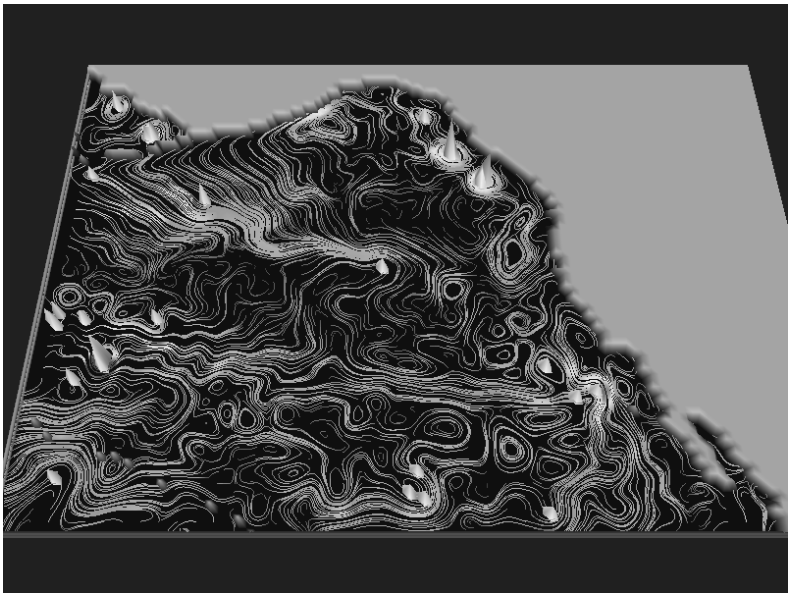

Fig. 3. Pacific Ocean with global streamlines and a white height field of the curvature centre density.

ever, in slightly elliptic flow (see Figure 4c), the peak is 'spread out' (see Figure 4d). This causes many missing peaks, and possibly also some false peaks.

4 The Winding-Angle Method

Another geometric method for detecting vortices in 2D, inspired by [7], builds upon the intuitive idea of a swirling pattern around a central set of points. The method tries to detect vortices by selecting looping streamlines and then clustering them. Selection is performed using a simplified winding-angle criterion and a distance criterion.

Let S_i be a 2D streamline, consisting of points $P_{i,j}$ and line segments $(P_{i,j}, P_{i,j+1})$, and let $\angle(A, B, C)$ denote the angle between line segments AB and BC. Then, the *winding-angle* $\alpha_{w,i}$ of streamline S_i is defined as the cumulative change of direction of the streamline segments:

$$\alpha_{w,i} = \sum_{j=1}^{N-1} \angle(P_{i,j-1}, P_{i,j}, P_{i,j+1}) \tag{1}$$

See Figure 5. We use signed angles, with positive rotation for a counterclockwise-rotating curve, and negative rotation for a clockwise-rotating curve. Obviously, $\alpha_{w,i} = \pm 2\pi$ for a fully closed curve; lower values may be used to find winding streamlines which do not make a full revolution.

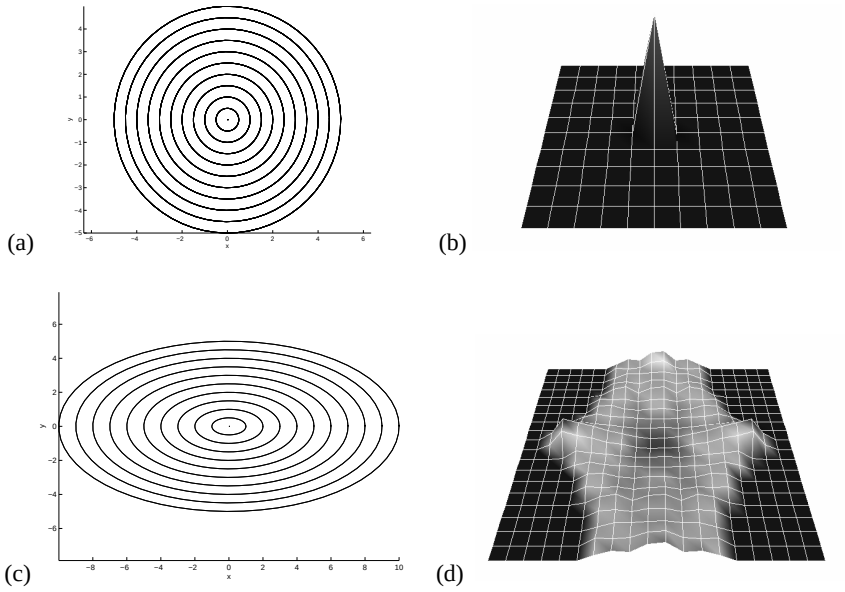

Fig. 4. In circular flow (a), there is a peak in the CCD field (b). In elliptic flow (c), the peak in the CCD field is spread out (d).

The selection process tries to find the streamlines that belong to a vortex by using two criteria: (1) the winding-angle of a streamline should be $k \cdot 2\pi$, with $k \geq 1$, and (2) the distance between the starting and final point of the streamline should be relatively close.

We have extended the work described in [12] from a visual, qualitative selection technique, to a more quantitative feature extraction technique. We now use the selected streamlines for automated vortex extraction and for determining numerical vortex attributes. This is done in two stages: *clustering* and *quantification*.

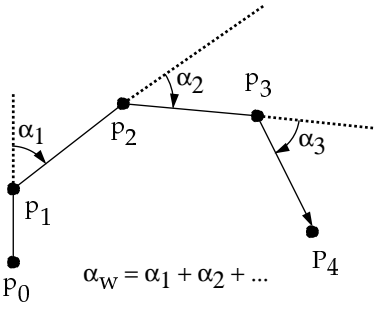

Fig. 5. The winding-angle $\alpha_{w,i}$ is the sum of the angles between the edges.

The purpose of *clustering* is to group those streamlines together which belong to the same vortex. Rather than clustering streamlines, it is easier to cluster points. To this end, each streamline is mapped to a point by determining the centre point, or geometric mean, of all sample points on the streamline. These centre points are then clustered as follows. The first cluster is formed by the first point. For each subsequent point, it is determined which previous cluster lies closest. If the point is not within a predetermined radius of all the existing clusters, it constitutes a new cluster. In this way,

the selected streamlines are combined into a distinct number of groups. Streamlines of the same group are considered to be part of the same vortex.

Once the streamlines have been clustered, *quantification* of the vortices is performed by calculating numeric attributes of the corresponding streamline clusters. We approximate the shape of the vortices by *ellipses*. Fitting an ellipse to a set of points is done by calculating statistical attributes, such as mean, variance, and covariance, of the points [8, 13]. In addition, we calculate specific vortex attributes, such as rotation direction and angular velocity. We denote the number of points on a streamline S_i as $|S_i|$, a cluster of streamlines as $C_k = \{S_{k,1}, S_{k,2}, \ldots\}$, where $S_{k,l}$ is streamline #l in cluster #k, the number of streamlines in that cluster as $|C_k|$, and all the points on all the streamlines in that cluster as $\Psi(C_k)$. Now, we can calculate the following attributes for each vortex:

- streamline centre: $\bar{S}_i = \frac{1}{|S_i|} \sum_{j=1}^{|S_i|} P_{i,j}$
- cluster centre: $\bar{C}_k = \frac{1}{|C_k|} \sum_{l=1}^{|C_k|} (\bar{S}_{k,l})$
- cluster covariance: $M_k = cov(\Psi(C_k))$
- ellipse axis lengths: $\boldsymbol{\lambda}_k = eig(M_k)$
- ellipse axis directions: $\mathbf{d}_k = eigvec(M_k)$
- vortex rotation direction: $d_k = sign(\alpha_{w,k})$
- vortex angular velocity: $\omega_k = \frac{1}{|C_k| \Delta t} \sum_{l=1}^{|C_k|} \alpha_{w,l}$

The vortices can be visualized by mapping their attributes to icons: the first three statistical attributes are used to calculate the axis lengths and directions of an ellipse which approximates the size and orientation of a vortex. The rotation direction of a vortex is visualized by small arrows. Finally, the angular velocity of a vortex is visualized by adding wheel spokes to the ellipse, the number of which is made proportional to the angular velocity: fast rotation is suggested by many spokes, slow rotation by few.

5 Results

5.1 The Bay of Gdańsk

The first example uses a data set of a simulation performed at WL | Delft Hydraulics of the Bay of Gdańsk, a coastal area in Poland. The goal of the simulation was to investigate the flow patterns induced by wind, the inflow of the Wisła (Vistula) river, and turbulence. The model is defined on a curvilinear grid of $43 \times 28 \times 20$ nodes, indexed by (i, j, k). Each node contains a 3D velocity vector $\mathbf{v}$, an eddy-diffusivity scalar E, and its gradient ∇E.

Figure 6 shows the result of applying the winding-angle method. The global flow patterns in the data set are visualized by the grey streamlines released from every grid node in a horizontal grid slice at the centre of the grid ($k = 9$). Selected streamlines are drawn in black. The ellipse icons visualize the approximate size and shape of the vortices, with the ellipse axes drawn in dashed lines. Arrows indicate the rotation direction of the vortices. The numbers of spokes indicate the strength of the vortices: the higher the number of spokes, the faster the rotation.

It can be seen that this method captures all visible vortices, including elongated and weak ones. An impression of the vortex strength (rotation speed) is immediately visible

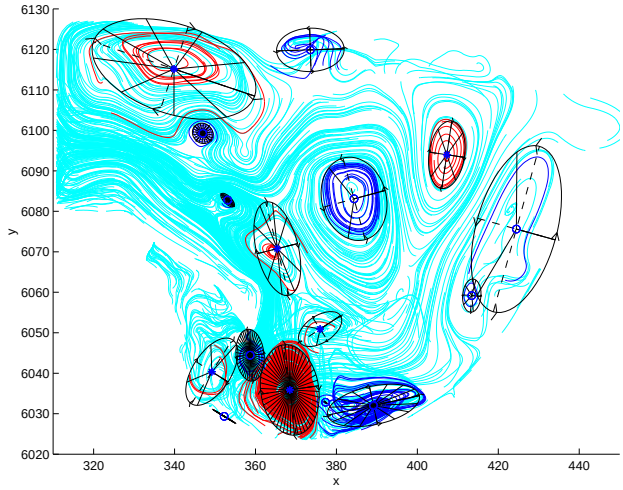

Fig. 6. Vortices in the Bay of Gdańsk. The number of spokes is proportional to ω.

from the number of spokes. It is also interesting to see that adjacent vortices rotate in opposite directions.

Figure 8 (see Appendix) shows a slightly different visualization, which uses rendered ellipses. Here, the angular velocity is not visualized, but the rotation direction of the vortices is indicated by the colour of the ellipses: red indicates clockwise rotation, and green counterclockwise rotation.

Once the vortices have been found, numerical attributes may be determined for each of them. Table 1 shows some of the results. Notice the differences between the largest and the smallest vortex (approx. factor 20), and between the fastest and the slowest one (approx. factor 15). There does not seem to be any correlation between the size and the rotation speed of the vortices.

number of clusters	15
number of CW vortices	5
number of CCW vortices	10
min. radius [km]	0.991
max. radius [km]	21.2
min. ω [s^{-1}]	5.3810^{-5}
max. ω [s^{-1}]	8.9310^{-4}

Table 1. Some numerical attributes of the vortices in the Bay of Gdańsk.

z-plane	#vortices	max λ_{CW}	max λ_{CCW}
16	1	-	0.5305
17	1	-	0.5832
18	1	0.6216	0.2076
19	2	0.8446	0.4968
20	2	1.1138	0.6117
21	1	0.9370	-

Table 2. Statistics of the vortices in the flow past a tapered cylinder.

5.2 Flow Past a Tapered Cylinder

The second example uses a data set of a simulation performed at NASA-Ames Research Center which concerns a laminar flow past a tapered cylinder [4]. This tapered cylinder has a variable radius depending on the z-coordinate, which influences the vortex shedding frequency at that height. The grid used is a structured, cylindrical grid with $64 \times 64 \times 32$ nodes, each of which contains density, x, y, z-momentum, and stagnation. The simulation is time-dependent, but we used only one time step.

We have applied the winding-angle method to extract vortices from six different z-slices, to show different patterns. Table 2 shows numerical statistics of these vortices, where $\max \lambda_{CW}$ is the maximum axis length of the clockwise vortex, and $\max \lambda_{CCW}$ of the counterclockwise vortex. It can be seen that for $z < 18$, there is only one counterclockwise vortex, for $18 \leq z \leq 20$, there are two vortices, rotating in opposite directions. For $z > 20$, the counterclockwise vortex has disappeared, leaving only a large clockwise vortex.

Figure 7 visualizes these slices, where the flow goes from left to right, past the cylinder which is drawn as a semi-circle on the left. Again, the global flow pattern is shown by grey streamlines, the selected streamlines are drawn in black, and the vortices are approximated by ellipse icons. Spokes indicate the rotation speed, and arrows the rotation direction

Figure 9 (see Appendix) shows a colour visualization of the slice at $z = 20$. As in the previous colour figure, the rotation direction of the vortices is indicated by the colour of the ellipses: green and red indicate opposite rotation. The grid slice has been coloured with the λ_2 scalar quantity. This quantity is defined as the second-largest eigenvalue of the tensor $S^2 + \Omega^2$, where $S = \frac{1}{2}(\nabla \mathbf{v} + (\nabla \mathbf{v})^T)$ and $\Omega = \frac{1}{2}(\nabla \mathbf{v} - (\nabla \mathbf{v})^T)$ are the symmetric and anti-symmetric parts of the velocity-gradient tensor $\nabla \mathbf{v}$. Highly negative values are supposed to indicate the presence of vortices [3]. However, in this example, the lowest (blue) values for λ_2 are observed at the front rather than behind cylinder, without any obvious vortices in the streamline pattern. Therefore, in this example, our winding-angle criterion turns out to be better than λ_2.

6 Conclusions and Future Work

We have described two geometric vortex detection methods. The curvature centre method has limitations similar to traditional methods. The winding-angle method is useful for finding both strong and weak vortices. Another important advantage is that it also allows for quantification, which leads to data reduction.

Future work includes incorporating critical points in the winding-angle method, to trace streamlines only in the neighbourhood of critical points, rather than globally in the entire field. Another useful application of the numerical attributes of vortices would be to perform spatial matching and temporal tracking of vortices. Matching and connecting ellipses found in adjacent (x/y/z) slices allows us to find 3D vortices, as long as they project reasonably to the slices. Temporal tracking allows us to study the evolution of vortices in time. Finally, we intend to extend the winding-angle technique to 3D. This is not trivial, because the winding-angle can be only determined in a 2D plane, and in vortices with a strong forward velocity component, it is not easy to choose such a plane.

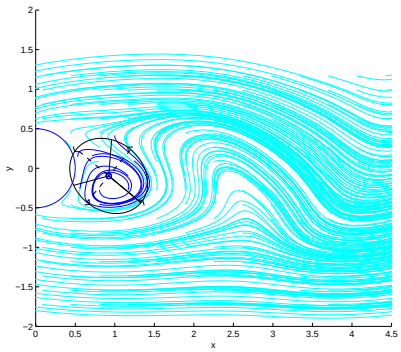

(a) z=16

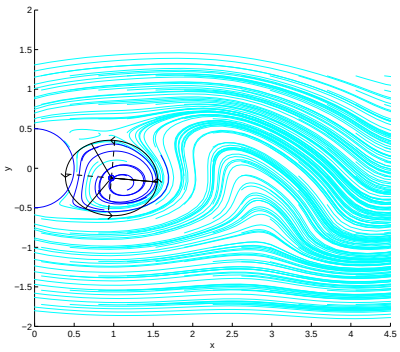

(b) z=17

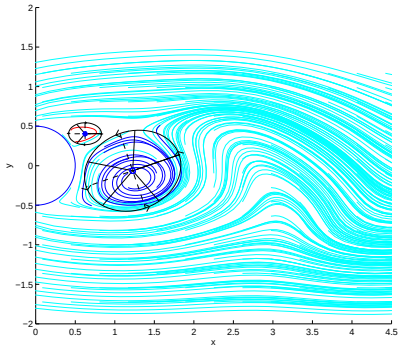

(c) z=18

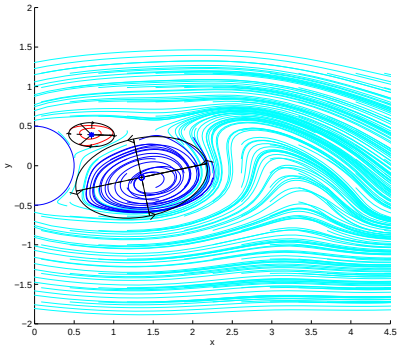

(d) z=19

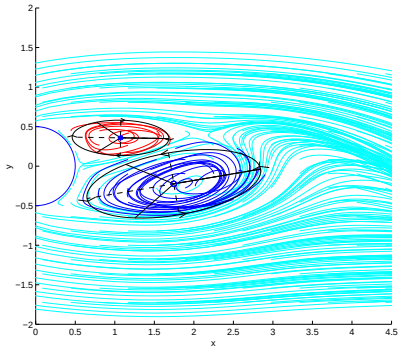

(e) z=20

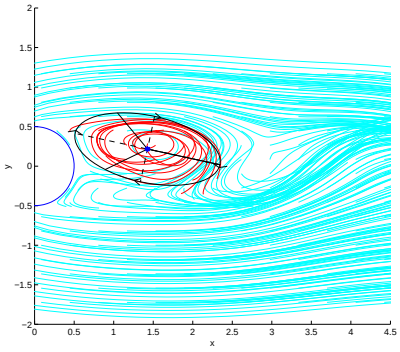

(f) z=21

Fig. 7. Flow past a tapered cylinder; different z-planes show different vortices.

Acknowledgment

We thank Freek Reinders for his efforts in preparing the visualization of the tapered cylinder.

References

1. D.C. Banks and B. A. Singer. A predictor-corrector technique for visualizing unsteady flow. *IEEE Transactions on Visualization and Computer Graphics*, 1(2):151–163, June 1995.
2. G. Farin. *Curves and Surfaces for Computer Aided Geometric Design*. Academic Press, 1990.
3. J. Jeong and F. Hussain. On the identification of a vortex. *Journal of Fluid Mechanics*, 285:69–94, 1995.
4. D.C. Jespersen and C. Levit. Numerical simulation of flow past a tapered cylinder. Technical Report AIAA 91-0751, NASA Ames R esearch Center, Reno, NV, January 1991. 29th AIAA Aerospace Sciences Meeting and Exhibit.
5. D. Kenwright and R. Haimes. Vortex identification - applications in aerodynamics: A case study. In R. Yagel and H. Hagen, editors, *Proc. Visualization '97*, pages 413–416, 1997.
6. W.C. de Leeuw and F.H. Post. A statistical view on vector fields. In M. Göbel, H. Müller, and B. Urban, editors, *Visualization in Scientific Computing*, Eurographics, pages 53–62, Wien, 1995. Springer-Verlag.
7. L.M. Portela. *On the Identification and Classification of Vortices*. PhD thesis, Stanford University, School of Mechanical Engineering, 1997.
8. F. Reinders, F.H. Post, and H.J.W. Spoelder. Feature extraction from Pioneer Venus OCPP data. In W. Lefer and M. Grave, editors, *Visualization in Scientific Computing '97*, pages 85–94, Wien, 1997. Eurographics, Springer Verlag.
9. M. Roth and R. Peikert. Flow visualization for turbomachinery design. In R. Yagel and G.M. Nielson, editors, *Proc. Visualization '96*, pages 381–384. IEEE Computer Society Press, 1996.
10. M. Roth and R. Peikert. A higher-order method for finding vortex core lines. In D. Ebert, H. Hagen, and H. Rushmeier, editors, *Proc. Visualization '98*, pages 143–150. IEEE Computer Society Press, 1998.
11. I.A. Sadarjoen. *Extraction and Visualization of Geometries from Fluid Flow Fields*. PhD thesis, Delft University of Technology, 1999.
12. I.A. Sadarjoen, F.H. Post, B. Ma, D.C. Banks, and H.G. Pagendarm. Selective visualization of vortices in hydrodynamic flows. In D. Ebert, H. Hagen, and H. Rushmeier, editors, *Proc. Visualization '98*, pages 419–423. IEEE Computer Society Press, 1998.
13. T. van Walsum, F.H. Post, D. Silver, and F.J. Post. Feature extraction and iconic visualization. *IEEE Transactions on Visualization and Computer Graphics*, 2(2):111–119, 1996.
14. Z.F. Zhu and R.J. Moorhead. Extracting and visualizing ocean eddies in time-varying flow fields. In *Proceedings of the 7th International Conference on Flow Visualization*, Seattle, WA, Sept. 1995.

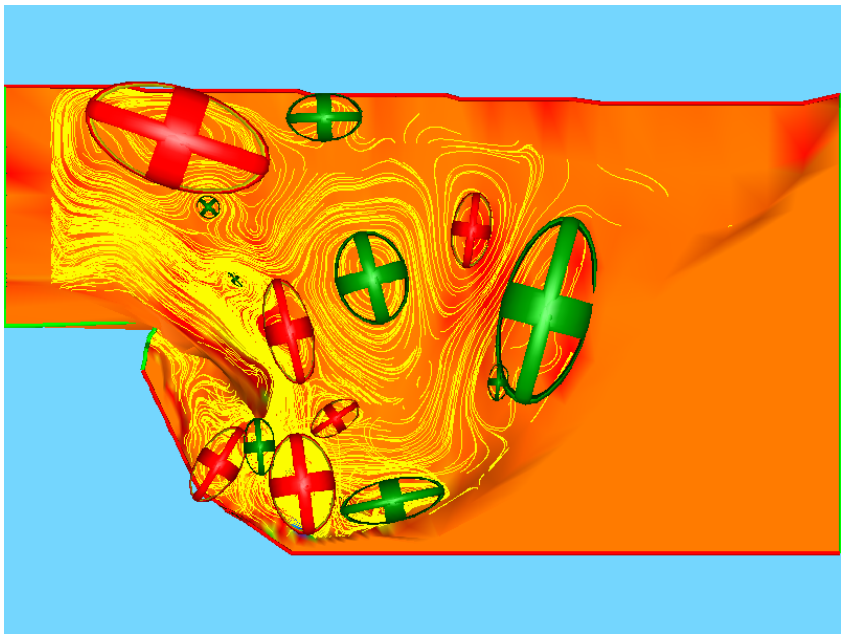

Fig. 8. Bay of Gdańsk with streamlines and vortices approximated by ellipses. Red and green indicate rotation in opposite directions.

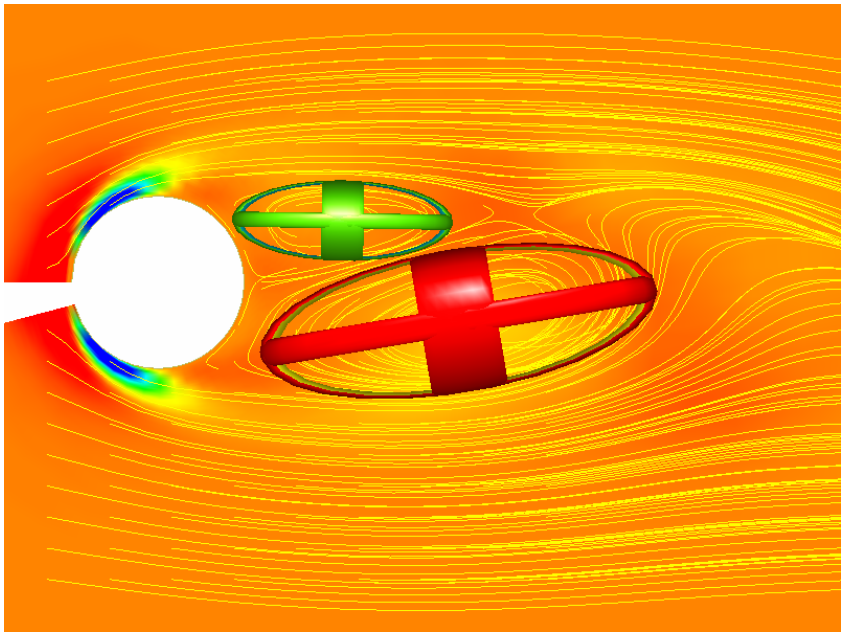

Fig. 9. Flow past a tapered cylinder with vortices approximated by ellipses, and streamlines released in a slice coloured with λ_2.